Original Article

Cite This: Colloid & Nanoscience Journal 2(4) (2025) 447-461.

CNJ.araku.ac.ir

Use of Fe_3O_4 Nanoparticles for Adsorption of Asphaltene from Heavy and Ultra-Heavy Materials: A Molecular Dynamics Study

Mohammad Reza Torki[1], Mojtaba Rahimi[1,2*], Maboud Hekmatifar[3]

Received: 2025-04-02
Revised: 2025-05-02
Accepted: 2025-05-04
DOI: 10.61186/CNJ.2.4.447

[1] Department of Petroleum Engineering, Kho.C., Islamic Azad University, Khomeinishahr, Iran

[2] Stone Research Center, Kho.C., Islamic Azad University, Khomeinishahr, Iran

[3] Department of Mechanical Engineering, Kho.C., Islamic Azad University, Khomeinishahr, Iran

Abstract

The asphaltene precipitation around the wellbore will result in formation damage, leading to a positive skin factor and an excess pressure drop during oil flow toward a production well or during water/gas flow away from an injection well. There are two solutions against asphaltene precipitation: treatment and inhibition. The conventional treatment methods are expensive and face limitations. Thus, the prevention of asphaltene precipitation is a much better solution. In recent years, there has been a growing interest in using nanoparticles (NPs) for asphaltene adsorption. Due to the unique properties of NPs in asphaltene adsorption (such as high surface-to-volume ratio and high adsorption tendency), they can inhibit the precipitation of asphaltene in the porous media, potentially mitigating the adverse effects of asphaltene precipitation on reservoir performance. This research employed molecular dynamics simulations to examine the influence of Fe_3O_4 NPs on the adsorption of asphaltene from heavy and ultra-heavy materials. A simulation duration of 10 ns was sufficient to achieve thermodynamic equilibrium in the initial atomic sample, with potential and total energy (TE) stabilizing at 5.16 and 6.06 kcal/mol at 300 K, indicating average attractive forces among the atoms. Based on the results, increasing Fe_3O_4 NPs concentration from 2.5 to 7% raised the diffusion coefficient from 0.51 to 0.61 Å²/fs and the mean square displacement (MSD) from 4.99 to 5.33 Å². However, further increasing the concentration to 10% resulted in a drop in the diffusion coefficient to 0.53 Å²/fs and a decrease in MSD to 5.06 Å². The maximum density profile of atomic structure rose from 0.0049 to 0.0055 atoms/Å³ at 7% concentration, but decreased to 0.0051 atoms/Å³ at 10%. Finally, the asphaltene adsorption rate improved from 72 to 79% as the concentration increased from 2.5 to 7%, but then dropped to 73% at 10%. These results highlight the optimal NP concentration for enhancing asphaltene adsorption without causing agglomeration issues.

Keywords: Asphaltene precipitation, Asphaltene adsorption, Fe_3O_4 nanoparticles, Molecular dynamics simulation.

1. Introduction

Crude oil, a vital energy source, comprises several compound groups, including paraffins, Naphthenes, aromatics, resins, and asphaltenes [1, 2]. Resins and asphaltenes, unlike the pure hydrocarbons of paraffins and aromatics, contain other elements like nitrogen (N), sulfur (S), oxygen (O), and metals like nickel and vanadium, forming NSO compounds. Asphaltenes are the heaviest constituents, prone to aggregation. Particles of asphaltene precipitate and aggregate into bigger structures known as clots under particular thermodynamic circumstances, such as temperature (Temp), pressure, and oil content. These clots deposit on rock surfaces and affect qualities like permeability and porosity [3, 4].

Corresponding author: Mojtaba Rahimi
Email: mrahimi@iau.ac.ir

Chemical additives like surfactants, polymer inhibitors, and adsorbents are effective in mitigating asphaltene deposition [4]. Adsorbents, such as beta zeolite, mineral surfaces (kaolin, calcite, dolomite), clay, reservoir rocks, and metal oxide nanoparticles (NPs) (e.g., MgO and titanium oxide) were employed [5, 6]. NPs are especially preferred for asphaltene adsorption because of their high surface-to-volume ratio, functional surface, and smaller size. This is because they boost transport in porous media and improve fluid flow performance during extraction [7-9]. The amount of asphaltene adsorbed on NPs hinges on NP's type, surface chemistry, and interaction forces with asphaltene [10, 11]. These forces encompass van der Waals force and polar acid-base interactions between NPs surfaces and asphaltene particles [12, 13]. Recent interest in NPs stems from their ability to efficiently adsorb asphaltene, contributing to enhanced crude oil properties [14, 15]. Nassar et al. [16] conducted a comprehensive investigation into the effect of six distinct NPs, namely ferrite, cobalt oxide, titanium oxide, MgO, CaO, and NiO, on asphaltene precipitation via the thermogravimetric method. Their findings revealed intriguing insights, particularly regarding the adsorption properties of CaO, which exhibited a notable adsorption capacity. However, intriguingly, it did not demonstrate the highest adsorption affinity under identical conditions. This observation suggests a lack of direct correlation between the highest adsorption capacity and the highest adsorption affinity within this context. Shojaati et al. [39] delved into the effects of ferrite NPs, nickel oxide, and γ-Al_2O_3 on the initiation of asphaltene precipitation. Their investigation highlighted the distinct behavior exhibited by NPs with varying chemical natures. It is important to note that NPs with Brønsted–Lowry acid sites and acidic chemical properties, as exemplified by γ-Al_2O_3, exhibited a greater propensity to delay the onset of asphaltene precipitation than NPs with an amphoteric chemical nature, such as ferrite. Sayyad Amin et al. [17] focused on examining the breadth of unstable and supersaturated zones of tarballs in the absence of NPs, employing the anti-solvent precipitation technique. The research conducted a thorough analysis of the effect of many elements on the supersaturation phenomena, such as the breadth of unstable zone, initial solute concentration, mixing area, and anti-solvent addition rate. Kulkarni and Myerson [18] conducted research centered on using functionalized NPs to modulate solubility within a given system. Their findings underscored a notable reduction in system solubility upon the addition of functionalized NPs, thereby elucidating the efficacy of such NPs in controlling solubility dynamics within the system. Lu et al. [19] embarked on an investigation into the effect of solvent composition on asphaltene adsorption behavior onto silica surfaces, employing molecular dynamic simulation techniques. In the framework of the SARA (saturation, aromatic, resin, asphaltene) model, their results provide insight into the complex interactions between asphaltene molecules and silica surfaces. They noticed, among other things, that asphaltene molecules had a propensity to interact in a T-shaped fashion with silica surfaces, which eventually resulted in the creation of thick asphaltene aggregates and provided important information about the mode of occurrence of base heavy oil. In petroleum engineering and materials science, investigating asphaltene adsorption processes in heavy and super-heavy materials is critical. Asphaltenes, complex organic compounds inherent in crude oil, play pivotal roles across various sectors of the petroleum industry, from production to transportation and refining. Understanding the behavior of asphaltenes, particularly their interaction with NPs, holds immense significance for optimizing industrial processes and enhancing resource utilization efficiency. Molecular dynamics (MD) simulation has become a potent instrument for investigating the complex dynamics of asphaltene-NPs interactions at the atomic level in recent years. Researchers acquired invaluable insights into the mechanisms that underlie asphaltene adsorption onto NP surfaces and have identified the factors that affect this phenomenon by utilizing MD simulations [20]. In this context, the present research aimed to explore the effect of Fe_3O_4 NPs on the asphaltene adsorption process in heavy and super-heavy materials using MD simulation techniques. By delving into this investigation, the study tried to shed light on the nuanced interactions between Fe_3O_4 NPs and asphaltene molecules, providing novel insights into the kinetics, thermodynamics, and mechanisms governing the adsorption process. Using advanced simulation techniques, this research tried to enhance the fundamental comprehension of asphaltene adsorption dynamics in heavy and super-heavy materials through innovative exploration. Consequently, it provided potential opportunities for the optimization of industrial processes within the petroleum industry [21]. In brief, the novelty of the research lies in examining the impact of various factors on the interaction between asphaltenes and surfaces using MD simulation methods. Specifically, this research investigates the following: 1) Change in the atomic ratio of nanoparticles: By altering the atomic ratio of nanoparticles, it is feasible to investigate how different compositions affect the adsorption of asphaltenes. This provides insight into the optimal configuration of NPs to prevent asphaltene precipitation; 2) Change in initial temperature: Studying the effect of different initial temperatures allows researchers to understand how

temperature influences the interaction between asphaltenes and surfaces. This knowledge can be used to optimize temperature conditions for controlling asphaltene aggregation and precipitation. By examining these aforementioned factors, this study contributes new insights into the behavior of asphaltenes at the atomic level and provides innovative approaches for mitigating the challenges associated with asphaltene aggregation and precipitation in the petroleum industry.

2. Molecular Dynamics Simulation

MD simulation utilizes computational modeling to represent particle interactions based on classical physics principles, providing a dynamic view of particle motion. This approach addresses the complexities inherent in molecular systems by employing computational techniques that harmonize experimental data with theoretical models. By solving Newton's equations of motion, MD simulations recreate the behaviors of particles as they evolve over time. This method involves calculating the forces acting on each particle, enabling detailed characterization and analysis of how systems change [22].

$$F_i = m_i a_i = -\nabla_i U = -\frac{dU}{dr_i} \tag{1}$$

The complex structures of molecules present significant challenges for traditional analytical methods due to their dynamic nature, influenced by factors, such as Temp, pressure, and chemical interactions. Therefore, numerical methods are essential for accurately modeling molecular dynamics. One of the most prominent approaches is the velocity-Verlet algorithm. Unlike simpler integration techniques, the velocity-Verlet algorithm excels in precisely tracking the trajectories of individual atoms over time. This high level of precision is achieved by using Taylor series expansions and Newton's laws of motion, allowing for a detailed depiction of particle movements and interactions within complex and dynamic molecular environments. Moreover, the velocity-Verlet algorithm is renowned for its stability and efficiency, making it ideal for long-term simulations where small errors can accumulate and distort results [23-25]:

$$r_i\left(\mathrm{t}+\ \Delta\mathrm{t}\right) = 2\ r_i\left(t\right) - r_i\left(t-\Delta t\right) + \left(\frac{d^2 r_i}{dt^2}\right)\left(\Delta t\right)^2 \tag{2}$$

$$v\left(t+\Delta t\right) = v\left(t\right) + \Delta t\, v\left(t\right) + \frac{\Delta t\left(a\left(t\right)+a\left(t+\Delta t\right)\right)}{2} \tag{3}$$

The accuracy of MD simulation relies heavily on the quality of the force field, which must be well-parameterized to model realistic physical and chemical behaviors. This force field evaluates particle interactions based on their spatial configurations and mutual effects, serving as the computational framework for the simulation. It meticulously calculates the forces acting on each particle, including electrostatic interactions, van der Waals forces, and covalent bonds, ensuring that particle movements and interactions align with real-world physical principles. [23].

$$E_{total} = E_{bonded} + E_{nonbonded} \tag{4}$$

This study delved into the intricate dynamics of particle interactions using discrete potential functions, notably focusing on the application of Lennard-Jones (LJ) and Coulomb potentials to model non-bonded interaction energy [26-28]. Within the LJ potential, a widely applied model in MD simulations, both repulsive and attractive components are encompassed, offering insights into the energy between neutral atoms or molecules relative to their spatial arrangement. While the repulsive aspect prevents particle overlap by accounting for electron cloud repulsion, the attractive facet captures van der Waals forces at extended distances [28].

$$U_{LJ} = 4\varepsilon\left[\left(\frac{\sigma}{r}\right)^{12} - \left(\frac{\sigma}{r}\right)^{6}\right] \qquad r < r_c \tag{5}$$

The ε_{ij} and σ_{ij} parameters play a pivotal role in unraveling the complexities of intermolecular interactions, serving as metrics for gauging the intensity and extent of attraction among the particles. These parameters are derived through meticulous computations and experimental investigations, offering invaluable insights into the intricate behaviors of molecules at a molecular level. A profound understanding of ε_{ij} and σ_{ij} not only guides the design of materials but also empowers the development of strategies aimed at finely tuning molecular interactions [29, 30].

$$\varepsilon_{ij} = \sqrt{\varepsilon_i \varepsilon_j} \tag{6}$$

$$\sigma_{ij} = \frac{\sigma_i + \sigma_j}{2} \tag{7}$$

The concept of electric potential energy, often referred to as electrostatic potential energy, is rooted in Coulomb's law, a fundamental principle in electromagnetism. According to Coulomb's law, the force between two charged particles is directly proportional to the product of their charges and inversely proportional to the square of distance among them. This principle governs the interactions among static electric charges within a given system. When multiple charged particles are present in a system, their positions relative to each other affect the distribution and magnitude of electric potential energy within that system. The electric potential energy represents the work performed by the electrostatic force in arranging these charges from their initial positions to their final configuration. Essentially, it quantifies the amount of energy stored in the system due to the arrangement of electric charges [26] :

$$U_{ij}(r) = \frac{-1}{4\pi\varepsilon_0} \frac{q_i q_j}{r_{ij}^{\ 2}} \tag{8}$$

2.1. Present simulation details

This study took a comprehensive approach to investigate the process of asphaltene adsorption within a simulated environment. The simulation box, representing the system under study, was set to the dimensions of 100 Å. Initially, key components of the system were modeled individually using specialized software tools. A substrate, mimicking a quartz crystal, was created at the bottom of the simulation box using Avogadro software. The solvent, consisting of water molecules, was modeled with the TIP3P model using LAMMPS software. Moreover, the structures of asphaltene (composed of 5S1N2O90H73C), Fe_3O_4, and zeolite ZSM-5 were constructed using Avogadro software. Subsequently, a mixture containing water, asphaltene, Fe_3O_4, and ZSM-5 zeolite was assembled on top of a quartz crystal surface using Packmol software. To achieve a realistic depiction, periodic boundary conditions were imposed in all directions, simulating an endless system. Following the initial setup, the conjugate gradient method was used to reduce the system's energy over 100,000 time steps, with the NVE ensemble keeping the volume, number of particles, and energy constant. Upon achieving energy minimization, the simulation transitions to the NVT ensemble, where the Temp was controlled using a Nose-Hoover thermostat.

The equilibrium of the modeled structure was then verified to ensure atomic stability. Once stability was confirmed, the focus shifted to investigating the process of asphaltene adsorption within the simulated system. Physical quantities relevant to the adsorption process were carefully monitored and reported. To capture the system's thermal behavior, atomic structures were sampled at regular intervals, with each time step set to 1 femtosecond. Thermal sampling occurred every 10,000-time steps to analyze changes in the system's configuration and behavior over time. Fig. 1 shows the schematic of the studied asphaltene structure.

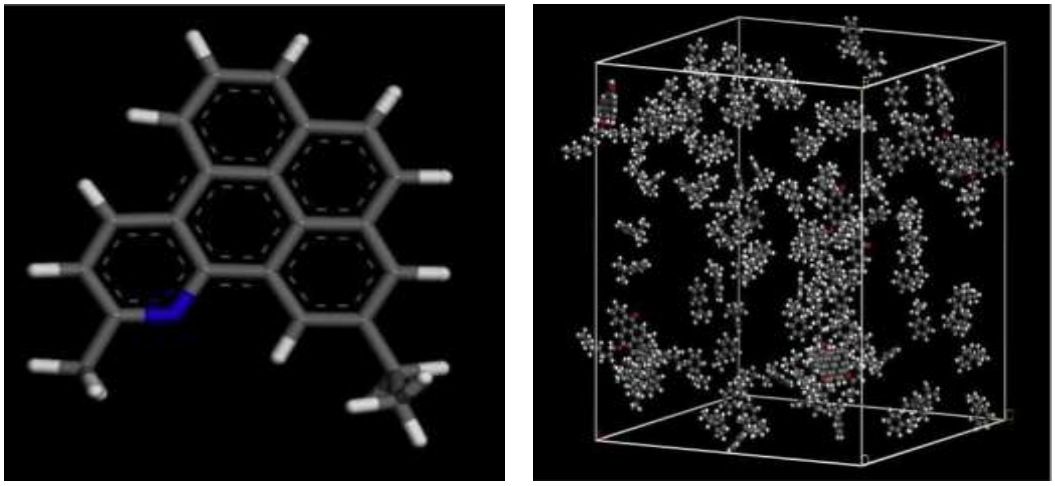

(a) (b)

Fig. 1 (a) Schematic of the studied asphaltene structure (grey, white, and blue colors represent carbon, hydrogen, and nitrogen atoms), and (b) expanded asphaltene structure in the simulation box.

3. Equilibration Process

Temporal changes in potential energy and the entire prototype were meticulously calculated to investigate the equilibrium process within the simulation box thoroughly. The numerical results of these quantities are depicted in Figs. 2-3. Fig. 2 reveals the changes in potential energy of the initial atomic sample at a Temp = 300 K, serving as the initial conditions for the molecular dynamics simulation. Numerically, the potential energy value within the simulated sample converged to 5.16 kcal/mol after 10 ns. This numerical convergence signified the presence of an average absorbent force across different regions of the simulation box, elucidating its structural integrity. Furthermore, the convergence of potential energy indicated saturation, implying stability in the atom positions within the simulated sample under the desired initial conditions. Consequently, it suggested the physical stability of the proposed atomic sample for practical applications.

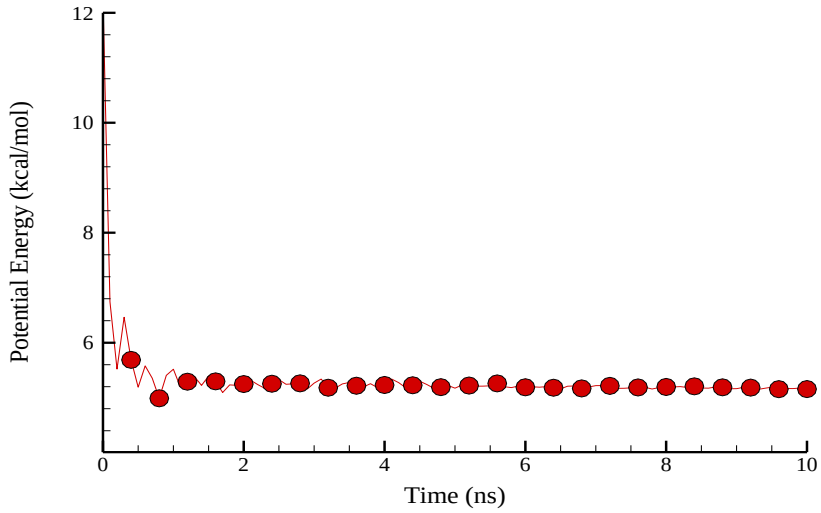

Fig. 2 Changes in the potential energy of the atomic sample as a function of time in the initial conditions at the initial Temp = 300 K.

In the following, the total energy (TE) changes were calculated according to the simulation time to better examine the thermodynamic equilibrium process in the primary atomic structure. The structure's TE value converged to approximately 6.06 kcal/mol as the simulation time progressed (Fig. 3). The sum of kinetic and potential energies in an atomic sample was the TE from a computational perspective. Consequently, the stabilization of the simulated sample was a result of the convergence of this parameter, which suggested an

equilibrium among the changes in kinetic and potential energies. This equilibrium was crucial for ensuring the reliability of simulation results. Another critical factor affecting the convergence of TE in atomic samples was the adjustment of Temp and pressure damping during the simulation. Proper calibration of these parameters ensured that the simulated sample reached a stable state, reflecting its structural stability under real-world conditions. The findings from this analysis demonstrated the effectiveness of the simulation setup in capturing the thermodynamic equilibrium process within the atomic structure. This process can be leveraged in practical applications, particularly in the adsorption and removal of asphaltene in industries, such as oil and petrochemicals.

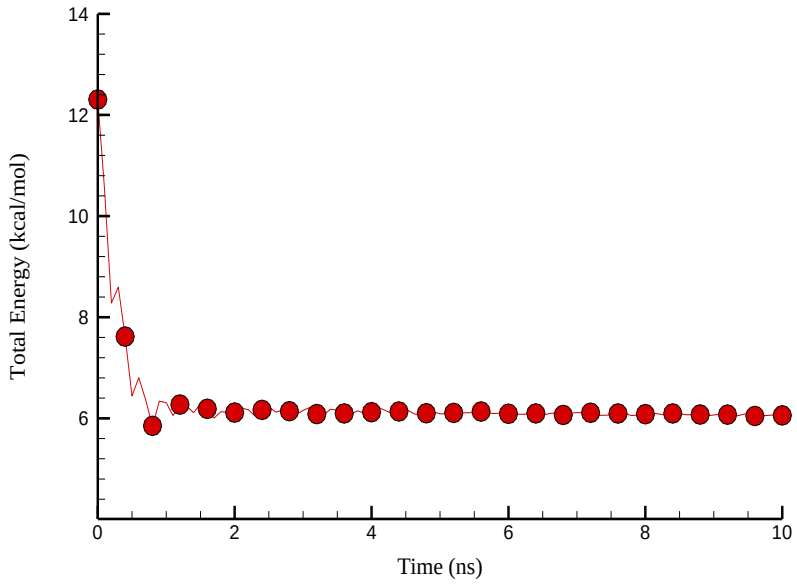

Fig. 3 TE changes of the initial atomic sample at Temp= 300 K as the initial conditions of MD simulation.

4. Radial Distribution Function

After achieving equilibrium in the atomic sample, the Radial Distribution Function (RDF) of the water environment within the simulation box was calculated and reported. The RDF is a crucial metric in atomic structures, indicating how atoms are spatially arranged under specific conditions and providing insights into the system's structural behavior. In this study, the RDF of the aqueous region at equilibrium, maintained at a Temp = 300 K, is depicted in Fig. 4. This function illustrates the probability of locating a particle at various distances from a reference particle, thereby mapping the spatial arrangement within the atomic structure. A comparison of the RDF obtained in this study with those from previous research showed a notable similarity. This consistency validated the appropriateness of simulation settings employed in the present study. The similarity between the RDF which resulted from this study and those from prior investigations confirmed the reliability of simulation parameters and methodologies. Such alignment served as a validation of the current calculation methods, demonstrating their accuracy. This validation via RDF analysis indicated that the simulation accurately captured the structural properties of the water environment under the specified conditions.

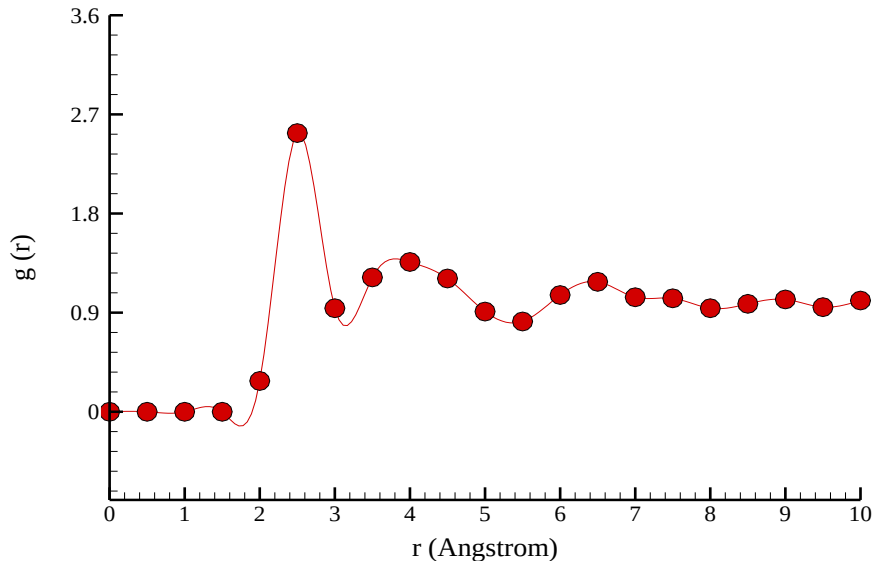

Fig. 4 The radial distribution function of the aqueous environment after equilibration in the sample during 10 ns.

5. Results and Discussion

5.1. Asphaltene adsorption process in atomically equilibrated samples

Various factors affect the efficiency and dynamics of adsorption in the structural adsorption process of asphaltene in an absorbent matrix. Mean square displacement parameters reflect asphaltene molecule movement within the matrix, impacting adsorption rate and quantity. Additionally, the diffusion coefficient controls asphaltene molecule speed within the matrix, while density changes affect molecule packing and distribution. The adsorption rate directly dictates how quickly asphaltene molecules are absorbed by the matrix. During post-equilibrium structure creation, the adsorption process is elucidated through mean square displacement, diffusion coefficient, density changes, and adsorption rate calculations. These parameters collectively shape the efficiency, kinetics, and extent of asphaltene structural adsorption, which is crucial for designing effective adsorption processes in industrial applications. The numerical outputs of the mean square displacement at different times at a Temp = 300 K and in a period of 10 ns are presented in Fig. 5. These results indicate successful structural transformation of asphaltene compared to the primary absorbent matrix, thus preventing phenomena such as asphaltene particle adhesion. In the process of asphaltene structural adsorption within the matrix absorber, the mean square displacement parameter characterizes the average squared distance traveled by individual atoms or molecules within the system over a specified time period from their original positions. This parameter offers valuable insights into the mobility and diffusion behavior of the atomic structure during the adsorption process. A higher mean square displacement value signifies greater mobility and diffusion of the atomic structure, indicating increased movement and potential diffusion of asphaltene molecules into the matrix. Numerically, the mean average displacement reaches 4.81 Å after 10 ns, highlighting the significant mobility and diffusion of the atomic structure during this period.

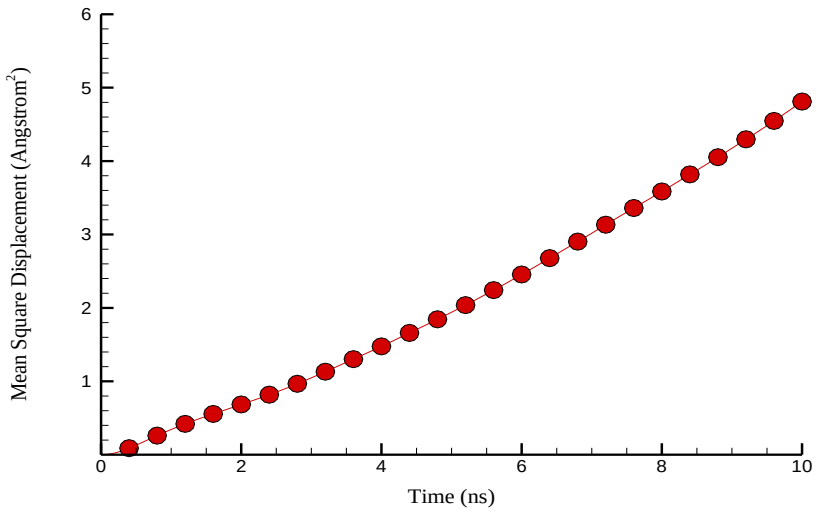

Fig. 5 The mean square displacement of the atomic structure at a Temp = 300 K and in a period of 10 ns.

The diffusion coefficient of atomic structure at a Temp = 300 K over a period of 10 ns is illustrated in Fig. 6. The velocity and extent of asphaltene molecules' interaction with the matrix materials are influenced by this parameter, which also determines their capacity to diffuse in the absorbent matrix. A higher diffusion coefficient indicates faster movement and diffusion of asphaltene molecules in the matrix, facilitating their adsorption and distribution throughout the material. Understanding and controlling the diffusion coefficient parameter is necessary to optimize the adsorption process, increase the efficiency of asphaltene removal, and design effective adsorbent materials for industrial applications. On the other hand, based on the obtained results, it can be said that the passage of more simulation time leads to a more intense transformation of the structure and a more effective separation of asphaltene from the initial solution. Based on the results of molecular dynamics simulation, the numerical value of the diffusion coefficient quantity reaches 0.482Å^2/fs after 10 ns.

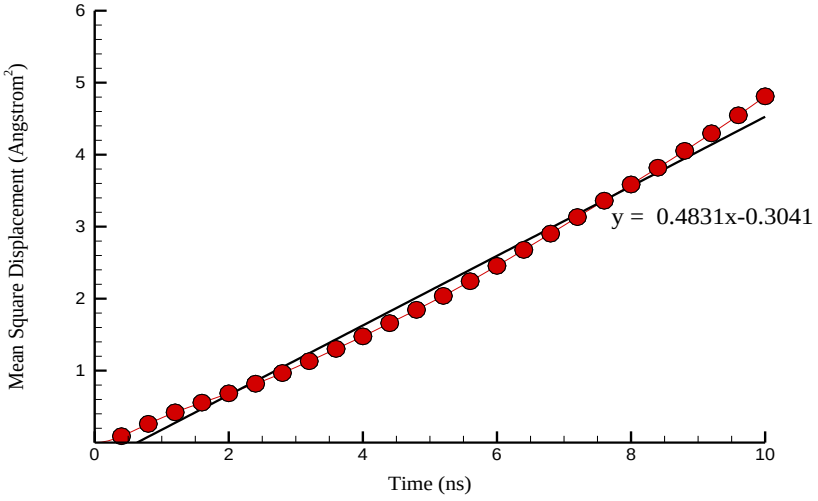

Fig. 6 The diffusion coefficient of the atomic structure at a Temp = 300 K and in a period of 10 ns.

The density profile and asphaltene adsorption rate were calculated and reported in the subsequent section to as effectively investigate the asphaltene adsorption process by the designed matrix. The asphaltene density profile is depicted in Fig. 7 at a Temp = 300 K and after 10 ns. Based on the obtained numerical profile, it can be said that the maximization of this profile in the middle part indicates the effective adsorption and placement of asphaltene in the vicinity of the absorbent matrix, so that the maximum density value in this simulation is equal to 0.0039 atm/Å^3. Therefore, the increased agglomeration of asphaltene molecules near the matrix surface is a result of the intense interaction between asphaltene molecules and absorbent matrix materials. This interaction can lead to the adsorption and agglomeration of asphaltene molecules in the middle part.

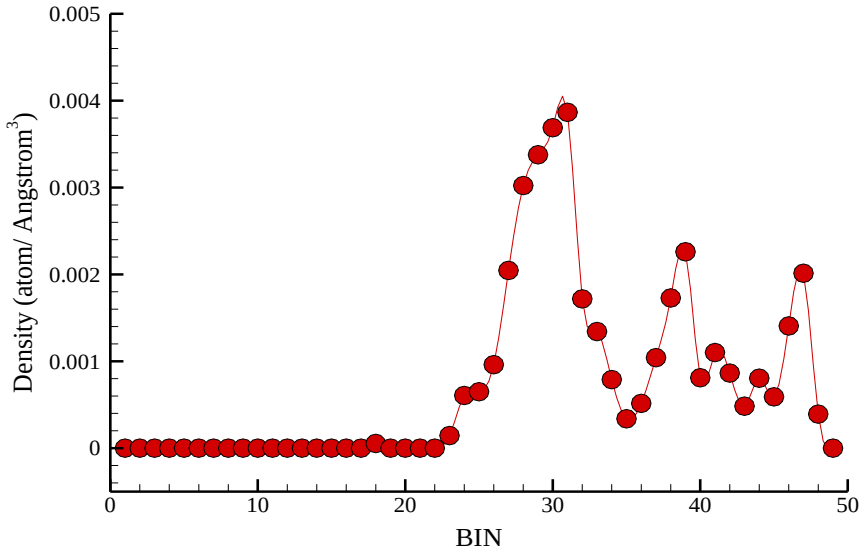

Fig. 7 Density profile of asphaltene molecules in the atomic structure at a Temp = 300 K and in a period of 10 ns.

Fig. 8 displays the level of asphaltene adsorption inside the atomic structure under the conditions of a Temp = 300 K and a period of 10 ns. To quantify the adsorption of asphaltene, a region with a detection boundary of 12 Å was identified and the quantity of asphaltene deposited was measured relative to the original matrix. The temporal progression of this measure with respect to the duration of the simulation is shown in Fig. 8. Numerically, the amount achieves a value of 69% during a time span of 10 ns. This numerical number will quantify the degree of asphaltene adsorption in the specified system during real-world operations. Over time, asphaltene molecules have more opportunities to contact the absorbent matrix, allowing for a greater number of interactions and adsorption events to occur. This long-term exposure leads to the gradual agglomeration of asphaltene molecules near the absorbent matrix, and as a result, adsorption increases in the vicinity of the matrix.

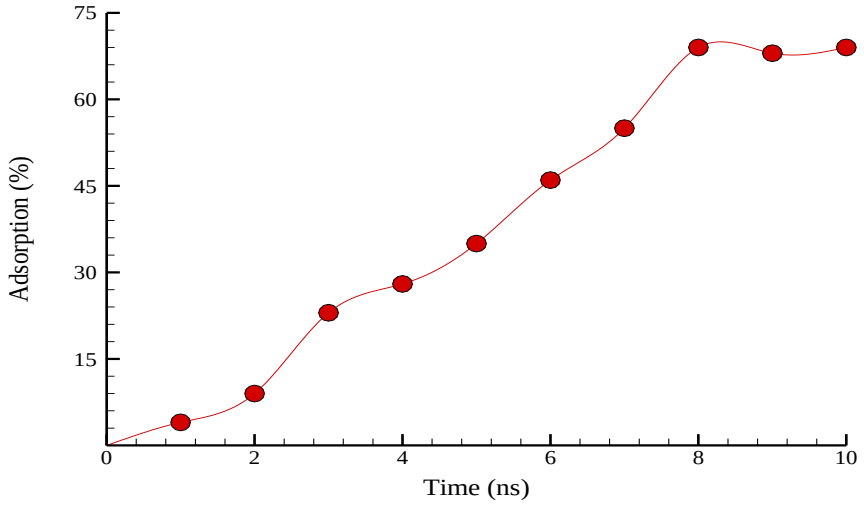

Fig. 8 The amount of asphaltene adsorption in the atomic structure in the present study at a Temp = 300 K and a duration of 10 ns.

5.2. The effect of Fe_3O_4 NPs on asphaltene adsorption process in equilibrated atomic samples

Previous studies showed that the presence of NPs may greatly affect the adsorption of different molecules by the absorbent matrix. To achieve this objective, Fe_3O_4 NPs with a 2.5% atomic ratio were introduced into the main absorbent matrix, and the simulations were then repeated. The results of MD simulations at this stage indicated the presence of proper physical equilibrium in these samples with the passage of time. As a result, it will be possible to use NPs in real cases without structural instability. Fig. 9 reveals the evolution of the simulated sample

structure in the presence of Fe_3O_4 NPs in the equilibration stage at the initial Temp = 300 K and in the presence of 2.5% of NPs.

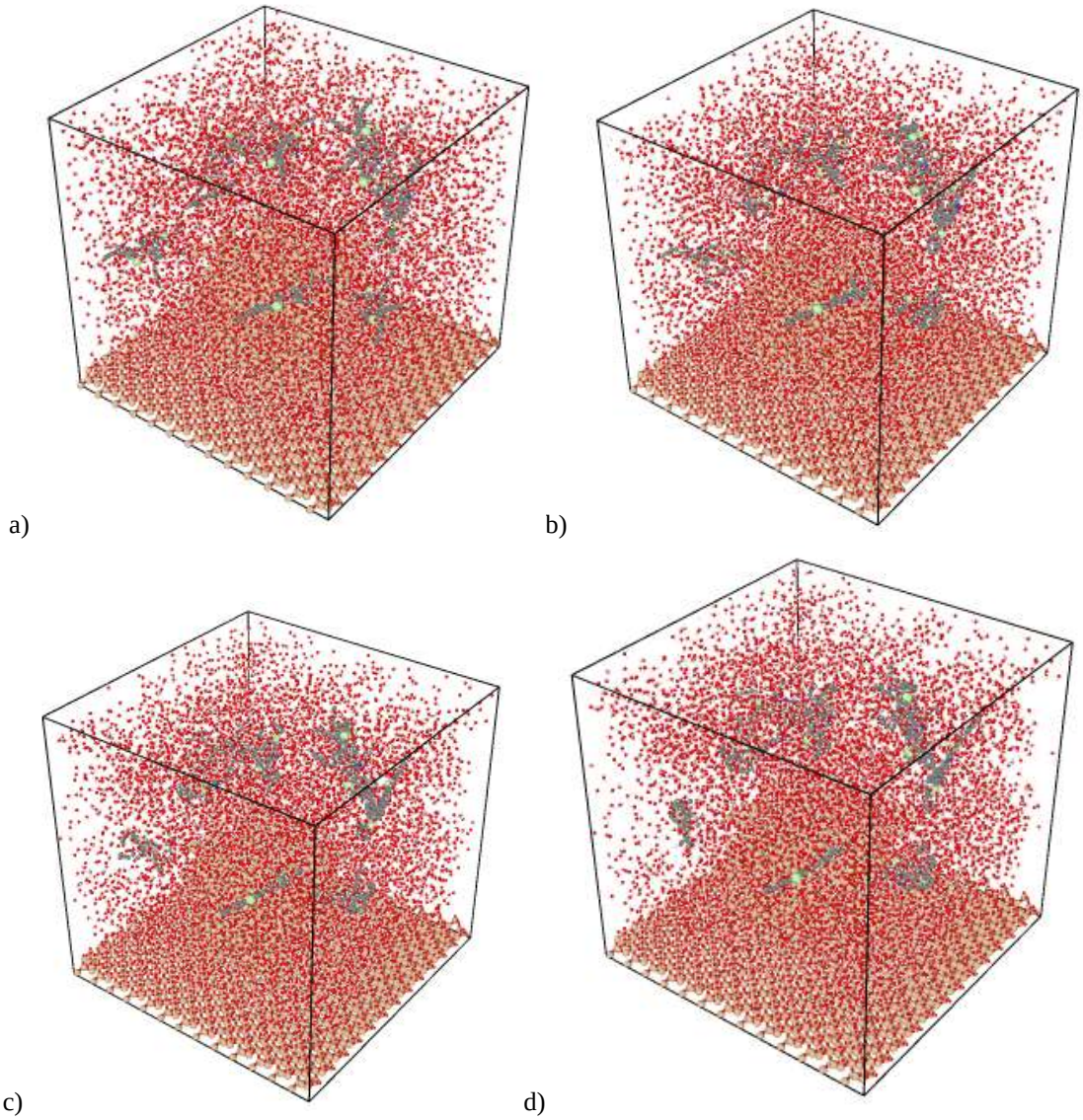

Fig. 9 The evolution of the simulated sample structure in the presence of Fe_3O_4 NPs in the equilibration stage and in the presence of 2.5% of NPs in different time steps a) 2.5 ns, b) 5 ns, c) 7.5 ns, and d) 10 ns.

Similar to the preceding section, the initial numerical assessments involved calculating the mean square displacement and diffusion coefficient to monitor structural evolution in the samples. Fig. 10 depicts the mean square displacement of the atomic structure in the presence of 2.5% NPs, at a Temp = 300 K, spanning a period of 10 ns. According to the graph in Fig. 10, the mean square displacement value increased steadily over time in the simulated sample, reaching 4.99 Å after 10 ns. MD simulations indicated that introducing NPs into the initial matrix amplified this mean square displacement value. The augmented mean square parameter of asphaltene displacement near the absorbent matrix, attributed to Fe_3O_4 NPs, arose from their size and surface properties impacting asphaltene molecule diffusion behavior. As Fe_3O_4 NPs integrated into the system, they interacted with asphaltene molecules, altering their movement and distribution around the absorbent matrix. Consequently, an

enhanced time evolution of asphaltene molecules was anticipated, leading to heightened proximity to the absorbent matrix, thereby improving their adsorption and removal. With the NPs concentration increasing from 2.5 to 7%, the mean square displacement parameter escalated from 4.99 to 5.33 Å. However, further NPs increment, up to 10%, induced a decrease in this parameter due to NPs concentration and clustering phenomena.

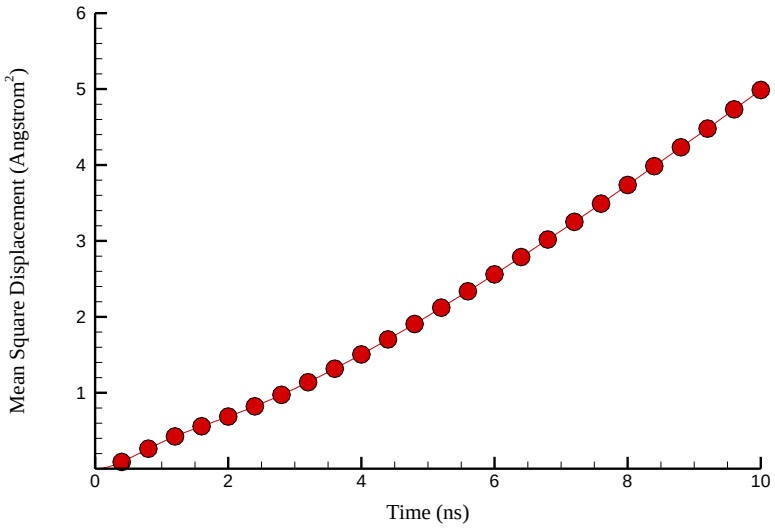

Fig. 10 The mean square displacement of the atomic structure in the presence of 2.5% NPs at a Temp = 300 K and in a period of 10 ns.

Fig. 11 portrays the diffusion coefficient of the atomic structure in the presence of 2.5% Fe3O4 NPs, at 300 K, over a duration of 10 ns. As depicted in Fig. 11, the diffusion coefficient in the devised sample amounts to 0.512 Å^2/fs, indicating a numerical increase compared to the preceding simulated sample. A more intricate and heterogeneous environment emerged upon the introduction of Fe_3O_4 NPs into the system, affecting the diffusion behavior of asphaltene molecules. The heightened diffusion coefficient parameter can be attributed to the NPs' ability to generate multiple pathways for asphaltene molecule movement. These NPs served as carriers or facilitators for asphaltene release, fostering unhindered and swifter molecule movement within the system. Increased movements led to a corresponding augmentation in the asphaltene diffusion coefficient parameter, as molecules covered greater distances within a given timeframe. Numerical findings revealed that by increasing Fe_3O_4 NPs from 2.5% to 7%, the diffusion coefficient in the analyzed sample escalated from 0.51 to 0.61 Å^2/fs, with the maximum value attained in the presence of 7% NPs.

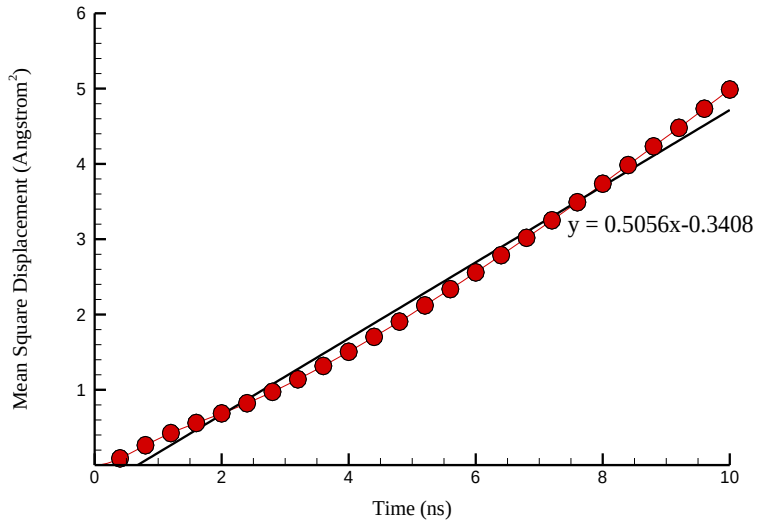

Fig. 11 The diffusion coefficient of the atomic structure in the presence of 2.5% of NPs at a Temp = 300 K and for a period of 10 ns.

The atomic structure's density profile at 300 K with 2.5% nanoparticles present is shown in Fig. 12. From a numerical perspective, the maximum density profile in the vicinity of the absorbent matrix's surface converged to 0.0049 atm/Å^3 by adding Fe3O4-NPs to the main matrix. This structural and temporal process led to an increase in the adsorption of asphaltene molecules. However, the improvement in the adsorption process expressed by helping NPs defined in the simulation box was more intense by increasing the amount of these NPs to 7%. This behavior occurred as a result of improving and optimizing the interaction energy (adsorbing force) between the designed matrix and asphaltene molecules.

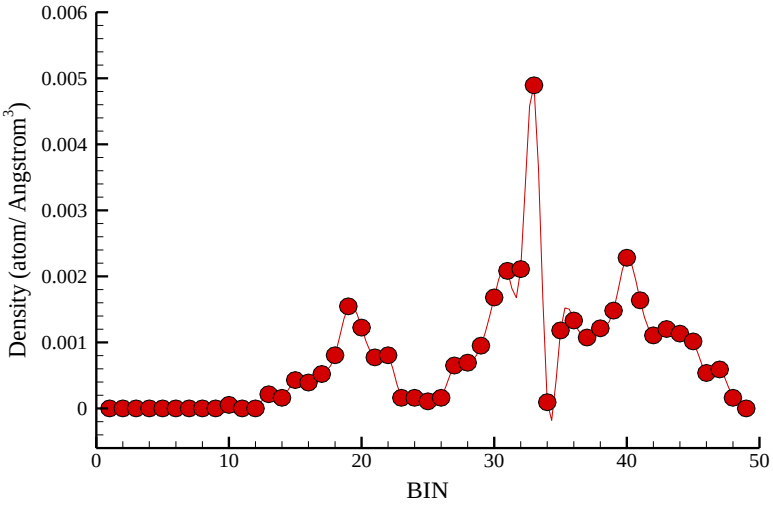

Fig. 12 Density profile of the atomic structure in the presence of 2.5% of NPs at a Temp = 300 K and for a period of 10 ns.

The quantity of asphaltene adsorption in the atomic structure is illustrated in Fig. 13 for a period of 10 ns at a Temp = 300 K and the presence of 2.5% of NPs. According to the diagram provided, the quantity of asphaltene adsorption increased as time passed. Additionally, the adsorption rate parameter increased from 72 to 79% as a result of the presence of NPs and the gradual increase in the quantity of Fe_3O_4 NPs from 2.5 to 7%. The concentration of NPs resulted in a decrease in the quantity of asphaltene adsorption to 73%, as a result of the

presence of larger quantities of NPs (10%). The increase in asphaltene adsorption in the structural adsorption process in an adsorbent matrix due to the presence of Fe_3O_4 NPs can be attributed to the increase in adsorption capacity and surface interactions facilitated by NPs from a technical perspective. When Fe_3O_4 NPs are introduced into the system, they can create a more favorable environment for asphaltene molecules to adhere to the adsorbent matrix and increase the overall adsorption capacity of the system. Besides, the presence of Fe_3O_4 NPs changes the surface properties of the adsorbent matrix and makes it more favorable for asphaltene adsorption.

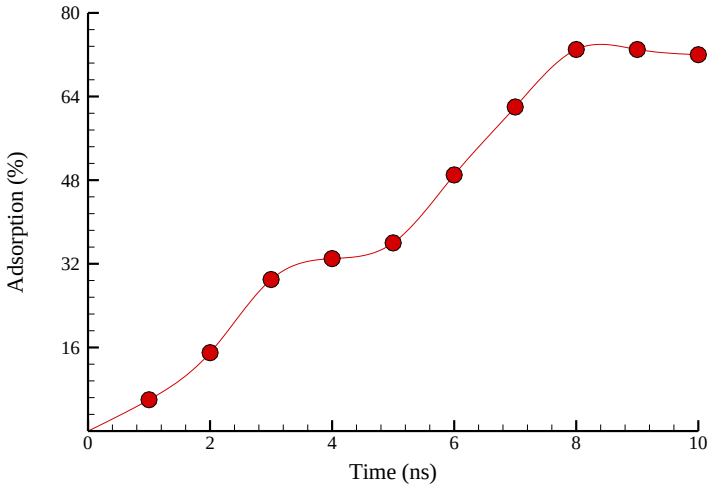

Fig. 13 The amount of asphaltene adsorption in the atomic structure in the presence of 2.5% of NPs at a Temp = 300 K and for a period of 10 ns.

The numerical outputs from molecular dynamics simulations, which include the mean square displacement, diffusion coefficient, maximum asphaltene density profile, and asphaltene adsorption rate during the adsorption process, are summarized in Table 1. These results are related to different atomic percentages of Fe_3O_4 NPs at 300 K over a duration of 10 ns, under the initial conditions specified in the study.

Table 1 Numerical outputs obtained in asphaltene adsorption process for different atomic values of Fe_3O_4 NPs.

Atomic ratio of Fe_3O_4 NPs (%)	Mean Square Displacement (Å²)	Diffusion Coefficient (Å²/fs)	Maximum Density Profile (atoms/Å³)	Asphaltene adsorption rate (%)
2.5	4.99	0.51	0.0049	72
5	5.12	0.56	0.0052	76
7	5.33	0.61	0.0055	79
10	5.06	0.53	0.0051	73

6. Conclusion

The conventional treatment methods of asphaltene precipitation are expensive and face limitations. Thus, the prevention of asphaltene precipitation is a much better solution. Owing to the outstanding properties of NPs in asphaltene adsorption (including high surface-to-volume ratio and high adsorption tendency), they can hinder the precipitation of asphaltene in the porous media, potentially mitigating the adverse effects of asphaltene precipitation on reservoir performance. In the present study, the MD method investigated the adsorption of asphaltene from heavy and ultra-heavy materials in the presence of Fe_3O_4 NPs. The simulations were performed for a total time of 20 ns and in the form of two main parts of equilibration of atomic samples and adsorption of asphaltene molecules. The results of the equilibration phase of the present study are summarized as follows:

- A duration of 10 ns was sufficient to achieve thermodynamic equilibrium in the initial simulated atomic sample.

- At 300 K, the potential energy and TE of the sample stabilized at 5.16 and 6.06 kcal/mol, respectively, indicating an average attractive force among the atoms in various regions of the simulation box.

After establishing equilibrium in the initial atomic sample, which indicated its structural stability, the simulation of the adsorption process of asphaltene molecules was carried out using a small focal ensemble for 10 ns, and the following results were obtained:

- Increasing the concentration of Fe_3O_4 NPs from 2.5 to 7% resulted in the diffusion coefficient rising from 0.51 to 0.61 Å²/fs.
- Increasing the concentration of Fe_3O_4 NPs from 7 to 10% resulted in the diffusion coefficient dropping from 0.61 to 0.53 Å²/fs.
- With an increase in Fe_3O_4 NPs from 2.5 to 7%, the Mean Square Displacement of atomic structure rose from 4.99 to 5.33 Å².
- With an increase in Fe_3O_4 NPs from 7 to 10%, the Mean Square Displacement of atomic structure decreased from 5.33 to 5.06 Å².
- The maximum density profile of the atomic structure increased from 0.0049 to 0.0055 atm/Å³ when the Fe_3O_4 NPs concentration increased from 2.5% to 7%.
- However, increasing the Fe_3O_4 NPs concentration from 7 to 10% led to a decrease in the Max density profile from 0.0055 to 0.0051 atoms/Å³.
- The asphaltene adsorption rate improved from 72 to 79% as the concentration of Fe_3O_4 NPs increased from 2.5% to 7%.
- The asphaltene adsorption rate decreased from 79 to 73% as the concentration of Fe_3O_4 NPs increased from 7% to 10%.

Conflict of Interests

The authors have no conflicts of interest to declare.

Author information

*Corresponding Author: Mojtaba Rahimi
Email: mrahimi@iau.ac.ir

References

[1] S. Alimohammadi, S. Zendehboudi, and L. James, A comprehensive review of asphaltene deposition in petroleum reservoirs: Theory, challenges, and tips, Fuel, 252 (2019), 753-791. https://doi.org/10.1016/j.fuel.2019.03.016

[2] S. Kashefi, M. N. Lotfollahi, and A. Shahrabadi, Investigation of asphaltene adsorption onto zeolite beta nanoparticles to reduce asphaltene deposition in a silica sand pack, Oil & Gas Sciences and Technology–Revue d'IFP Energies nouvelles, 73 (2018) https://doi.org/10.2516/ogst/2017038

[3] G. Raj, E. Larkin, A. Lesimple, P. Commins, J. Whelan, and P. e. Naumov, In situ monitoring of the inhibition of asphaltene adsorption by a surfactant on carbon steel surface, Energy & fuels, 33(3) (2019) 2030-2036. https://doi.org/10.1021/acs.energyfuels.8b04246

[4] S. Kashefi, A. Shahrabadi, M. N. Lotfollahi, and A. Varamesh, A new polymeric additive as asphaltene deposition inhibitor in CO_2 core flooding, Korean Journal of Chemical Engineering, 33 (2016) 3273-3280. https://doi.org/10.1007/s11814-016-0199-y

[5] S. Wang, Q. Liu, X. Tan, C. Xu, and M. R. Gray, Adsorption of asphaltenes on kaolinite as an irreversible process, Colloids and Surfaces A: Physicochemical and Engineering Aspects, 504 (2016) 280-286. https://doi.org/10.1016/j.colsurfa.2016.05.086

[6] T. Pernyeszi, Á. Patzkó, O. Berkesi, and I. Dékány, Asphaltene adsorption on clays and crude oil reservoir rocks, Colloids and Surfaces A: Physicochemical and Engineering Aspects, 137 (1998) 373-384. https://doi.org/10.1016/s0927-7757(98)00214-3

[7] N. N. Nassar, Asphaltene adsorption onto alumina nanoparticles: kinetics and thermodynamic studies, Energy & Fuels, 24(8) (2010) 4116-4122. https://doi.org/10.1021/ef100458g

[8] C. Franco, E. Patiño, P. Benjumea, M. A. Ruiz, and F. B. Cortés, Kinetic and thermodynamic equilibrium of asphaltenes sorption onto nanoparticles of nickel oxide supported on nanoparticulated alumina, Fuel, 105 (2013) 408-414. https://doi.org/10.1016/j.fuel.2012.06.022
[9] A. W. Marczewski and M. Szymula, Adsorption of asphaltenes from toluene on mineral surface, Colloids and Surfaces A: Physicochemical and Engineering Aspects, 208 (2022) 259-266. https://doi.org/10.1016/s0927-7757(02)00152-8
[10] H. Alboudwarej, D. Pole, W. Y. Svrcek, and H. W. Yarranton, Adsorption of asphaltenes on metals, Industrial & engineering chemistry research, 44(15) (2005) 5585-5592. https://doi.org/10.1021/ie048948f
[11] N. N. Nassar, A. Hassan, and P. Pereira-Almao, Effect of the particle size on asphaltene adsorption and catalytic oxidation onto alumina particles, Energy & fuels, 25(9) (2011) 3961-3965. https://doi.org/10.1021/ef2008387
[12]B. Mirzayi and N. N. Shayan, Adsorption kinetics and catalytic oxidation of asphaltene on synthesized maghemite nanoparticles, Journal of Petroleum Science and Engineering, 121 (2014) 134-141. https://doi.org/10.1016/j.petrol.2014.06.031
[13] Y. Kazemzadeh, S. E. Eshraghi, K. Kazemi, S. Sourani, M. Mehrabi, and Y. Ahmadi, Behavior of asphaltene adsorption onto the metal oxide nanoparticle surface and its effect on heavy oil recovery, Industrial & Engineering Chemistry Research, 54(1) (2015) 233-239. https://doi.org/10.1021/ie503797g
[14] S. I. Hashemi, B. Fazelabdolabadi, S. Moradi, A. M. Rashidi, A. Shahrabadi, and H. Bagherzadeh, On the application of NiO nanoparticles to mitigate in situ asphaltene deposition in carbonate porous matrix, Applied Nanoscience, 6 (2016) 71-81. https://doi.org/10.1007/s13204-015-0410-1
[15] N. N. Nassar, A. Hassan, and P. Pereira-Almao, Effect of surface acidity and basicity of aluminas on asphaltene adsorption and oxidation, Journal of colloid and interface science, 360(1) (2011) 233-238. https://doi.org/10.1016/j.jcis.2011.04.056
[16] N. N. Nassar, A. Hassan, and P. Pereira-Almao, Metal oxide nanoparticles for asphaltene adsorption and oxidation, Energy & Fuels, 25(3) (2011) 1017-1023. https://doi.org/10.1021/ef101230g
[17] J. Sayyad Amin, S. Nikkhah, S. Zendehboudi, and L. A. James, Effective method to determine supersaturation of tar balls deposited along the Caspian sea, Energy & Fuels, 29(5) (2015) 2931-2939. https://doi.org/10.1021/ef502534w
[18] S. A. Kulkarni and A. S. Myerson, Reversible control of solubility using functionalized nanoparticles, Chemical communications, 53(8) (2017) 1429-1432. https://doi.org/10.1039/c6cc09390f
[19] N. Lu, X. Dong, Z. Chen, H. Liu, W. Zheng, and B. Zhang, Effect of solvent on the adsorption behavior of asphaltene on silica surface: A molecular dynamic simulation study, Journal of Petroleum Science and Engineering, 212 (2022) 110212. https://doi.org/10.1016/j.petrol.2022.110212
[20] A. S. Al Qasim, Simulation of asphaltene deposition during CO_2 flooding, 2011.
[21] N. Eskandari, Asphaltene deposition simulation in porous media during CO_2 injection using Lattice Boltzmann Method, Doctoral dissertation, Memorial University of Newfoundland, 2020.
[22] B. J. Alder and T. E. Wainwright, Studies in molecular dynamics. I. General method, The Journal of Chemical Physics, 31(2) (1959) 459-466.
[23] D. C. Rapaport and D. C. R. Rapaport, The art of molecular dynamics simulation. Cambridge university press, 2004.
[24] Q. Spreiter and M. Walter, Classical molecular dynamics simulation with the Velocity Verlet algorithm at strong external magnetic fields, Journal of Computational Physics, 152(1) (1999) 102-119. https://doi.org/10.1006/jcph.1999.6237
[25] E. Hairer, C. Lubich, and G. Wanner, Geometric numerical integration illustrated by the Störmer–Verlet method, Acta numerica, 12 (2003), 99-450. https://doi.org/10.1017/cbo9780511550157.006
[26] P. G. Huray, Maxwell's equations. John Wiley & Sons, 2009.
[27] M. S. Daw and M. I. Baskes, Embedded-atom method: Derivation and application to impurities, surfaces, and other defects in metals, Physical Review B, 29(12) (1984) 6443.
[28] J. E. Lennard-Jones, Cohesion, Proceedings of the Physical Society, 43(5) (1931) 461.
[29] A. K. Rappé, C. J. Casewit, K. Colwell, W. A. Goddard III, and W. M. Skiff, UFF, a full periodic table force field for molecular mechanics and molecular dynamics simulations, Journal of the American chemical society, 114(25) (1992) 10024-10035. https://doi.org/10.1021/ja00051a040

[30] S. L. Mayo, B. D. Olafson, and W. A. Goddard, DREIDING: a generic force field for molecular simulations, Journal of Physical chemistry, 94(26) (1990). https://doi.org/10.1021/j100389a010